Cloud frequency climatology at the Andes/Amazon transition: 1. Seasonal and diurnal cycles

Kate Halladay,[1] Yadvinder Malhi,[1] and Mark New[1,2]

Received 13 March 2012; revised 25 September 2012; accepted 5 October 2012; published 1 December 2012.

[1] Tropical montane regions present a complex local climate but one that may be very sensitive to local and global change. Therefore, it is important to assess their current climatological state, and to understand how the large-scale circulation may affect local-scale cloud patterns. We examine the cloud climatology of a tropical Andean montane region in the context of tropical South American climate in terms of seasonal/diurnal cycles using a corrected ISCCP (International Satellite Cloud Climatology Project) DX cloud product (1983–2008), MODIS (Moderate Resolution Imaging Spectroradiometer) MOD35 visible cloud flags (2000–2008) and ground-based cloud observations. Cloud climatologies were compared for three elevation zones: highlands (puna grassland), eastern slope (the montane forest) and lowlands. We found that in the dry season (JJA) the study area is part of a localized region of higher cloud frequency relative to other parts the eastern slope, and also relative to the adjacent highlands and lowlands. The highlands exhibited the greatest amplitude mean annual cycle of cloud frequency, with a minimum in June for all times of day. There were contrasts between the three zones with regard to the month in which the minimum cloud frequency occurs between different times of day. Higher lowland and eastern slope cloud frequencies compared with those on the puna in the early hours in the wet season suggest low-level convergence at lower elevations. Comparisons between satellite products show that ISCCP and MODIS produce very similar annual cycles although the absolute cloud frequencies are higher in ISCCP data.

Citation: Halladay, K., Y. Malhi, and M. New (2012), Cloud frequency climatology at the Andes/Amazon transition: 1. Seasonal and diurnal cycles, *J. Geophys. Res.*, *117*, D23102, doi:10.1029/2012JD017770.

1. Introduction

[2] Tropical Montane Cloud Forests (TMCFs) are a habitat of great importance to biodiversity as they contain a large number of species, many of which are endemic. TMCFs are defined by their almost constant immersion in cloud, the presence of which is controlled by topography and meteorological variables, usually where the prevailing wind encounters a mountain slope and is forced to ascend, leading to condensation and cloud formation. With the current and anticipated changes in climate, meteorological variables such as humidity and wind in addition to temperature may be affected, and therefore cloud distributions may be subject to change.

[3] The existing and potential impacts of climate change on TMCF ecosystems have been highlighted by *Foster* [2001] and *Pounds et al.* [1999] among others. *Pounds et al.* [1999] reported species decline in the Monteverde cloud forest in Costa Rica, which correlated with increasing tropical sea surface temperatures (SSTs). Widespread increases in SSTs increase latent heat release, decreasing the temperature lapse rate and thus increasing the height of the lifting condensation level (LCL). The LCL is the height at which moisture condenses if lifted adiabatically and equates to a theoretical cloud base height. Other studies have attempted to quantify this shift for various sites in the tropics [*Still et al.*, 1999], for Costa Rica [*Karmalkar et al.*, 2008], and for the Amazonian lowlands [*Pinto et al.*, 2009], since a change in cloud height will reduce the cloud frequency at one level while increasing it at another level. However, assessing the effect of increased surface temperatures on overall cloud frequency is a separate question. In addition, the complexity of cloud/climate feedbacks and the indirect effects of circulation changes mean that the individual regions need to be examined separately.

[4] This study focuses on a region in southeastern Peru at the transition from the high Andes to the Amazon rain forest, between which the vegetation changes from high-elevation grasslands (known locally as 'puna') through TMCF and sub-montane forest to lowland forest [*Rapp and Silman*, 2012]. In order to assess the extent of any changes in cloud

[1]Environmental Change Institute, School of Geography and the Environment, University of Oxford, Oxford, UK.
[2]African Climate and Development Initiative, University of Cape Town, Rondebosch, South Africa.

Corresponding author: K. Halladay, Environmental Change Institute, School of Geography and the Environment, South Parks Road, University of Oxford, Oxford OX1 3QY, UK. (kate.halladay@ouce.ox.ac.uk)

0148-0227/12/2012JD017770

distributions in this region, and to understand the mechanisms that are responsible for effecting those changes, it is necessary to characterize the current cloud climatology.

[5] Previous work in the area of interest has focused on summer (DJF) cloudiness (which is synonymous with cloud frequency in this context). *Garreaud and Wallace* [1997] examined the diurnal cycles of convective cloudiness across northern South America using passive satellite data from ISCCP (International Satellite Cloud Climatology Project) and microwave data at 0.5 degree resolution. On the eastern slope of the subtropical Andes, late afternoon and early morning maxima in convective cloud were found. The latter were attributed to low-level convergence. More recently, *Killeen et al.* [2007] and *Giovannettone and Barros* [2009] have used geostationary satellite imagery to identify variations in the diurnal cycle of convective cloudiness at different elevations in the central Andes. *Giovannettone and Barros* [2009] emphasized the role of topography in addition to the SST-driven large scale circulation in controlling convective cloudiness in southern Peru and the central Andes. *Killeen et al.* [2007] also comment on the distribution of regions of high mean cloud frequency in relation to wind direction and topography. In areas where the Andes are orientated approximately east-west, low-level northwesterly winds (known as the South American Low-Level Jet) impinge more directly on the slope and are forced upwards promoting convection. The South American Low-Level Jet (SALLJ) refers to the curving of the northeasterly trades by the Andean topography, so that they acquire a northwesterly trajectory over the lowlands to the east of the central Andes. *Nair et al.* [2008] used MODIS (Moderate Resolution Imaging Spectroradiometer) cloud mask data to produce cloud immersion maps for the Monteverde TMCF and analyzed the effect of the angle between prevailing winds and the slope, in relation to cloud frequency. They found that when the prevailing wind is parallel to the slope, areas of cloud immersion are more fragmented than when prevailing winds impinge directly on the slope. An analysis of the cloud frequency climatology in another TMCF region in Ecuador was undertaken by [*Bendix et al.*, 2004, 2006], however, the region is sufficiently far from the study area that circulation patterns and seasons are somewhat different such that similarities cannot be assumed.

[6] The climatology of convective cloud is closely related to that of precipitation. The strong influence of zonal wind anomalies on precipitation variability in this area on diurnal to interannual timescales [e.g., *Garreaud*, 1999; *Vuille*, 1999; *Vuille and Keimig*, 2004] is well known. *Vuille and Keimig* [2004] extend earlier analyses by showing that the controls on interannual variability differ between northern and southern regions of the Altiplano, notably that low-level moisture conditions over the lowlands to the east are of little significance to the variability of northern regions, i.e., close to the study area. Rossby waves from the extratropics are known to play a role in influencing the position and strength of zonal wind anomalies [*Lenters and Cook*, 1999; *Vuille et al.*, 1998].

[7] Little research has been undertaken on the specifics of the cloud climatology of the study area in the dry and transition seasons, in which the presence of low cloud becomes critical to the TMCF. Moreover, the focus of many previous studies has been on cold convective cloud as a proxy for rainfall. This type of cloud would not necessarily result in cloud immersion at the altitude of the TMCF.

[8] Therefore this study aims to:

[9] (1) Describe the cloud climatology of the study area, and place this in the regional context;

[10] (2) Examine the differences in the mean annual cycle and variability between the three zones found across the Andes/Amazon transition (i.e., the higher elevation grasslands, TMCFs on the eastern slope and lowland forest);

[11] (3) Examine the differences in the diurnal cycle between the three zones through the annual cycle;

[12] (4) Relate these aspects of the cloud climatology to the large-scale circulation and cloud formation mechanisms.

[13] A separate paper [*Halladay et al.*, 2012] presents an analysis of interannual variability and trends in cloud frequency of the study area. While focusing on a specific study region, this study aims to draw wider regional insights into the cloud climatology of the Andes-Amazon transition region. Section 2 describes the data and methods used, Section 3 describes the cloud climatology in terms of seasonal and diurnal cycles, while discussion and conclusions follow in Sections 4 and 5.

1.1. Study Area

[14] At the center of the study is the Kosñipata Valley (13.1°S, 71.5°W) in southeastern Peru, on the edge of the Manú National Park, which is a designated UNESCO World Heritage Site for biodiversity. This area is located within a narrow zone extending approximately northwest-southeast along the eastern flank of the tropical Andes, and has been a location of intensive ecological research since the late 1990s (e.g., *Malhi et al.* [2010] and subsequent papers in the same volume). The gradient of the eastern slope in this area is very steep as the altitude drops from approximately 3500 m to around 500 m over only 40 km (Figure 1b, digital elevation data from USGS GTOPO30), hence the climatic zones and their related ecosystems are restricted in extent. The TMCF is located in this narrow zone. To the west are the drier grasslands of the "*puna*" at altitudes of around 3500 to 4000 m, which also extend north and south in a much broader zone than the TMCFs, especially to the south where the Andes splits into eastern and western Cordilleras, either side of the Altiplano (15 to 21°S). The valleys of the eastern slope open out toward the northeast into the lowlands at around 1200 m beyond which altitude gradually reduces over Amazonia.

2. Data and Methods

[15] To obtain cloud observational data with the most complete spatial and temporal coverage, cloud frequency data sets from MODIS and ISCCP were extracted, as ground-based observations are scarce and confined to the last 10 years in the region of interest. However, ground-based observations of cloud amount that are available were used to compare with the satellite data.

2.1. MODIS Cloud Mask Data

[16] The MODIS polar orbiting satellites pass over the study area at approximately 13 to 14 UTC (2000 to present) and 18 to 19 UTC (2002 to present). Data from the MOD35 product were obtained for these times, over a 1 × 1 degree latitude/longitude area centered on San Pedro in the Kosñipata

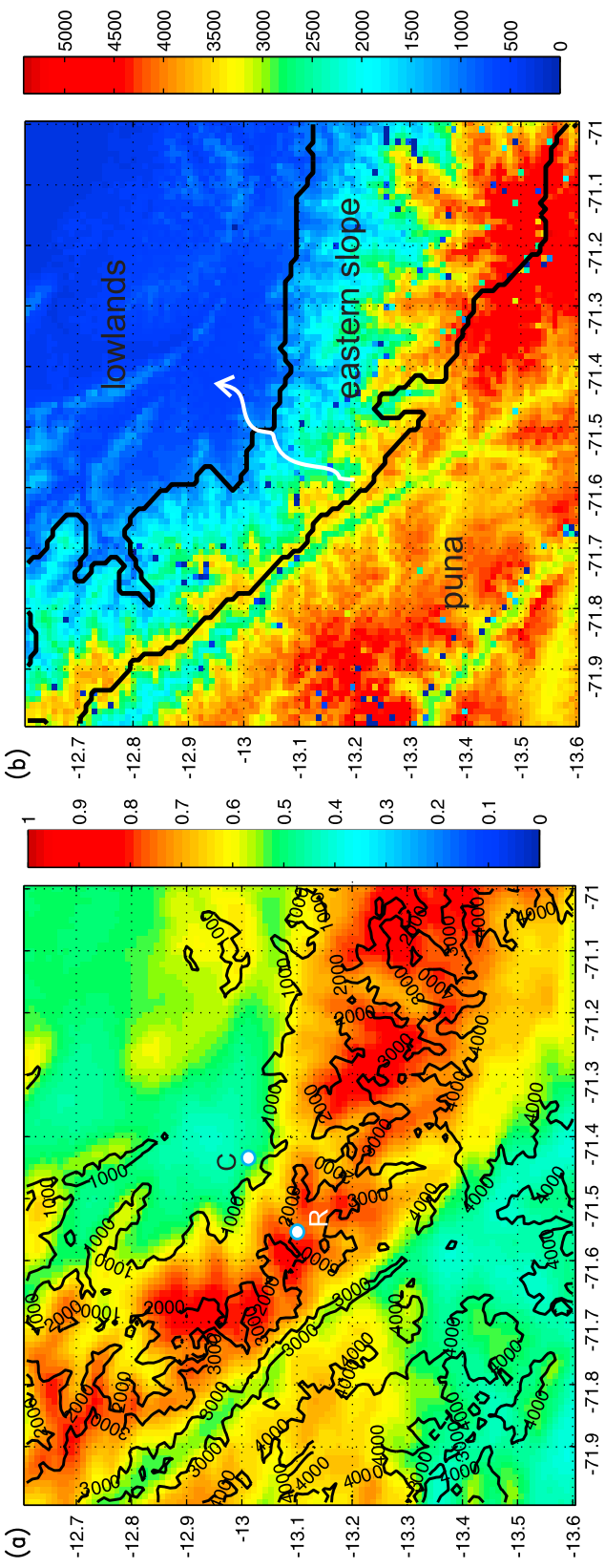

Figure 1. (a) Mean annual cloud frequency for 2000–2009 from MODIS MOD35 at 1 km resolution for a 1 degree by 1 degree area centered on the Kosñipata Valley, with Rocotal (R) and Chontachaca (C) meteorological stations marked, and (b) GTOPO30 Digital Elevation Model regridded to 1 km resolution with the eastern slope region enclosed by the solid black line. Terrain heights are in meters. Approximate extent of Kosñipata Valley is indicated by white line.

Valley (area shown in Figure 1), with a post-processing conversion from swath to a regular lat/long grid.

[17] The MOD35 product includes a 250 m resolution cloud mask derived from radiances at visible wavelengths, such that each 250 m pixel is assigned a 1 or a 0 for each overpass [*Ackerman et al.*, 2006]. Visible wavelengths are appropriate for the detection of low clouds which are not always identified at infrared wavelengths because their brightness temperature is very similar to that of the underlying surface. Therefore, for this study, the 250 m visible flags were extracted. When extracting the data, the determined/non-determined flag for each 1 km pixel (highest resolution available for quality control) was queried in order to reject pixels for which the algorithm was not executed owing to poor quality data. For each "determined" 1 km pixel, the 16 binary values were averaged to generate a single value for each 1 km pixel and each time step, which represented the cloud frequency for that pixel. Visible wavelengths sometimes detect clouds erroneously over snow, ice or open water; however, over vegetation, such as in this study area, this should not occur. MOD35 also includes the 1 km cloud mask, which assigns one of 4 categories to each pixel. In the processing applied to generate gridded products from the cloud mask, Hubanks *et al.* [2008] assign a cloud frequency of 0 to the classes "confident clear" and "probably clear" and 1 to the classes "uncertain" and "cloudy." With this approach, random comparisons were undertaken over the Kosñipata region as part of this study between visible images, the cloud mask, and output from the 250 m flags. These indicated some missed detections of high, thin cloud by the 250 m flags, and missed detection of low cloud by the cloud mask. However, in the context of moisture input to cloud forests, high, thin cloud is of limited relevance, hence only the 250 m data from MODIS were used in the analysis.

2.2. ISCCP Data

[18] The International Cloud Climatology Project [*Rossow and Schiffer*, 1991, 1999] is a collection of passive geostationary and polar-orbiter imagery from the period 1983 to 2008 processed into a number of gridded products (http://isccp.giss.nasa.gov/products/products.html). It is the longest continuous satellite record for cloud. For this study the DX (Pixel Level Cloud Product) cloud flag data (including all cloud types) were extracted for the period 1983 to 2008 for all GOES satellites. These data are available at 30 km and 3-hourly resolution. The geostationary instruments are usually located at 75°W and 135°W (GOES East and West positions, respectively), although over the period of the ISCCP data set, some eight GOES satellites have been operational. The cloud detection algorithm [*Rossow and Garder*, 1993] uses a visible wavelength in combination with the infrared window as these were found to be common to all the instruments that were assimilated by the project. Although the spatial resolution of this product is coarser than that of the MODIS product, it provides 8 images per day as opposed to two from MODIS, so it is more suited to analysis of the diurnal cycle. Furthermore, the data cover a period of 25 years enabling more robust statistics to be generated.

2.2.1. Viewing Angle Correction

[19] Some studies have questioned the suitability of the ISCCP data set for use in examining long-term trends in cloud frequency [e.g., *Evan et al.*, 2007], on the grounds that the cloud amount detected can be affected by the viewing angle of the satellite; the cloud-free areas in a field of view are less visible at oblique angles owing to the vertical dimension of the clouds. This is sometimes referred to as the 'geometric effect' [*Joyce et al.*, 2001; *Minnis*, 1989], and it increases the amount of cloud that is detected for these scenes. In the case of polar-orbiting satellites, this difference is averaged out as the viewing angle will change every few days. However, a geostationary satellite will view the same area from the same angle, unless it is repositioned. Therefore, over time, biases in cloud amounts detected between regions may arise and, if satellites are moved, inhomogeneities may be created. In this study, a correction for viewing angle was applied, based on that proposed by *Campbell* [2004]; the approach is fully described in the auxiliary material.[1]

2.3. Other Data

[20] In order to examine the large-scale circulation features at the surface and at upper levels that might influence the cloud climatology, the NCEP-NCAR reanalysis data [*Kalnay et al.*, 1996] were extracted. When examining large-scale, multiyear mean circulation patterns, there were no significant differences between NCEP-NCAR and ERA reanalyses, so only the former is used here. These data are available at 6-hourly and 2.5 by 2.5 degree resolution, for the period 1948 to present. Additionally, surface observations of cloud amount in oktas made daily by observers at 1200, 1800 and 0000 UTC (0700, 1300 and 1900 local time) were obtained from the Peruvian meteorological service (Senamhi) in Cuzco for two sites in the Kosñipata Valley area: Chontachaca (13.02°S, 71.47°W, elevation: 982 m) and Rocotal (13.11°S, 71.57°W, elevation: 2010 m). Chontachaca is located in the lowlands zone but close to the edge of the eastern slope and Rocotal lies approximately in the center of the eastern slope zone within the Kosñipata Valley. Observations were available for the period from January 2000 to December 2008. If any days from a month were missing, data from that month were excluded from the time series. Missing observations totaled 1% for Chontachaca, and 13% for Rocotal.

3. Results

3.1. Cloud Climatology: Mean Annual Cloud Frequency

[21] Figure 1a shows mean annual cloud frequency over the study region, and clearly illustrates the band of high cloud frequency (>0.6) that characterizes the eastern slope region. The lower altitude limit of this region of high cloud frequency coincides approximately with the 1500 m contour and the upper limit with a ridge of altitude 3000–3500 m in the northwest portion of the map. The highest mean annual cloud frequencies (>0.8) are found on exposed ridges oriented down the slope itself at altitudes of approximately 2000 to 3500 m (Figure 1). Above 4000 m, the cloud frequency begins to decrease again. The lower limit of the band of maximum cloud frequency likely reflects the climatological LCL, assuming that the cloud is mostly orographic and cloud base intersects the terrain. Under this assumption,

[1] Auxiliary materials are available in the HTML. doi:10.1029/2012JD017770.

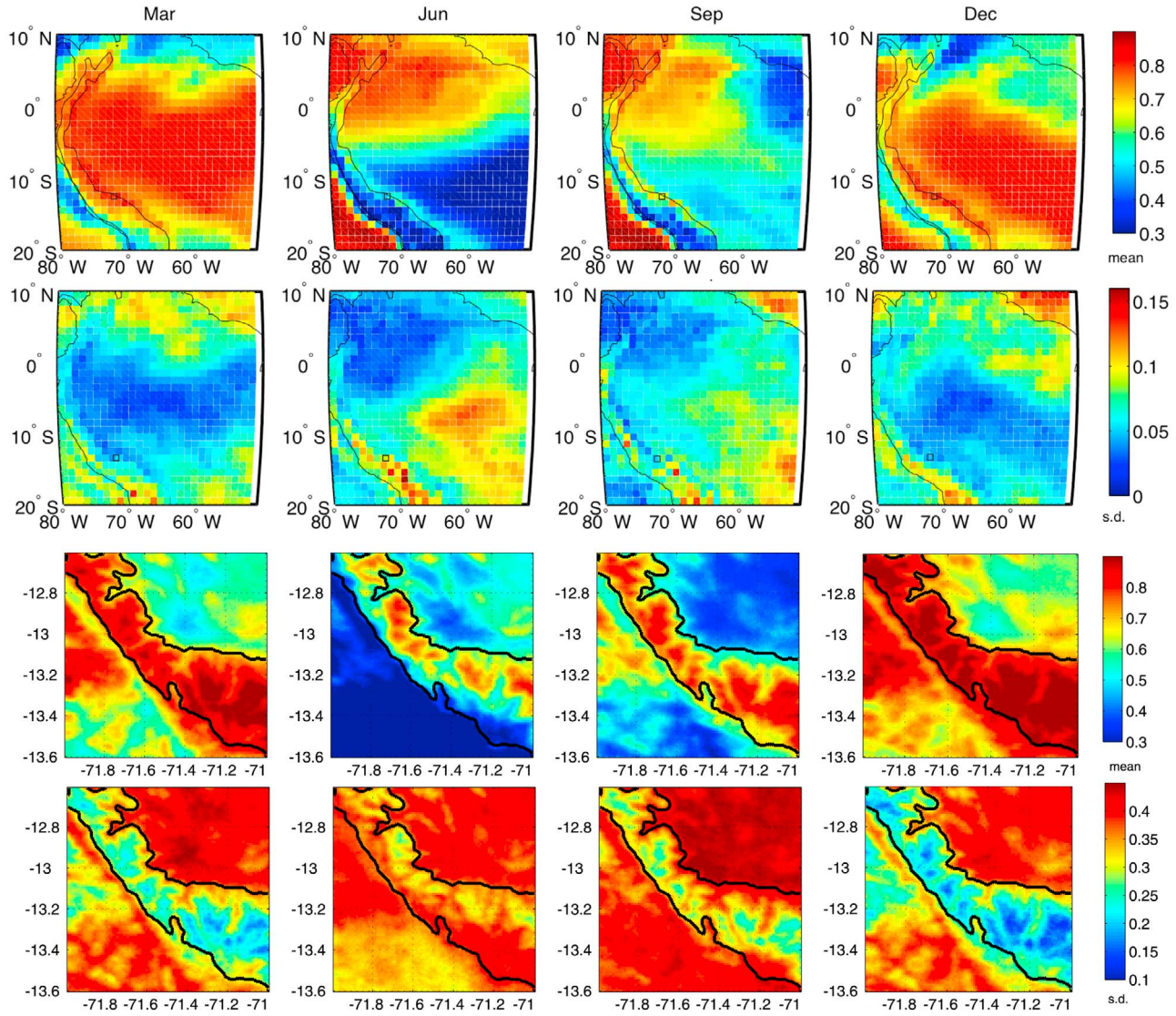

Figure 2. First row: mean cloud frequency by month at Amazon scale from ISCCP DX product 1983–2008, corrected. Includes data at 3-hourly intervals. Second row: as in first row but standard deviation. One degree × 1 degree region is marked by black box. Third row: mean cloud frequency by month at local scale from MODIS MOD35 visible cloud flags for passes at 0900 and 1400 local time (UTC-5), period 2000 to 2009. Eastern slope enclosed by solid black line. Fourth row: as in third row but standard deviation.

the upper limit of the band indicates the climatological cloud top height.

[22] The black line in Figure 1b encloses the "eastern slope" region used in this study, which is defined as areas with a mean annual cloud frequency greater than 0.65 in the 1 degree by 1 degree area shown on the map, but excluding any smaller regions isolated from the main slope. The area to the northeast of this slope region is defined as "lowlands," and the area to the southwest is defined as "puna."

3.2. Cloud Climatology: Seasonal and Diurnal Cycles of Cloud Frequency

3.2.1. Regional Cloud Frequency

[23] To place the Kosñipata Valley in a regional context, the annual cycle of cloud frequency from the ISCCP DX product across northern South America is illustrated in Figure 2 (first row). This cycle is similar to that of precipitation. In the southern and eastern areas, the period of minimum cloud frequency begins in May and persists until September, while northwestern areas experience high cloud frequencies linked to the northernmost position of the ITCZ. From October, the focus of convective activity moves south and eastward and by peak austral summer covers much of Amazonia, before retreating north and westward in austral autumn [*Horel et al.*, 1989] Throughout the year, a narrow band of high cloud frequency persists along the eastern slope of the Andes. In the early and late wet season months (March and December in Figure 2), the band becomes less distinct, almost merging with the main area of convection over the lowlands. In the mid and late dry season (June and September), the cloud frequency within this band still exceeds 0.6, in contrast with the adjoining regions to the northeast and

southwest. In June, and to a lesser extent in the other months the region around the study area has a higher mean cloud frequency compared with the eastern slope areas to the north and south. Standard deviations calculated using monthly time series over the 25 year period (Figure 2, second row) show that the eastern slope is also a region of low variability, which is approximately coincident with the areas of high mean cloud frequency and persists through all seasons. Coefficient of variation maps (not included) showed a similar pattern.

[24] Figure 2 (third row) illustrates the seasonal cycle of cloud frequency in the study area from MODIS MOD35. Areas of highest cloud frequency on the eastern slope, where mean annual cloud frequency exceeds 0.8, are the areas of greatest cloud frequency during all months of the year. In January (not shown), peak cloud frequencies occur for all areas, although the absolute values are higher on the puna than over the lowlands. The minimum cloud frequencies occur in June for the puna, in July for the eastern slope and in August for the lowlands. An area of consistently low cloud frequency is found in the lowlands at approximately 12.9°S, 71.4°W where the slope changes orientation. The standard deviations maps for the study area using monthly time series over a 10 year period (Figure 2, fourth row) show that the eastern slope has lowest variability and that the lowest variability tends to coincide with highest mean cloud frequency, as shown in the regional standard deviation maps. On the puna and lowlands the lowest variability often coincides with the highest mean.

3.2.2. The Seasonal Cloud Cycle on the Puna, Eastern Slope and Lowlands

[25] Figure 3 compares the cloud frequencies from ISCCP DX, MODIS MOD35 visible cloud flags and cloud observations from surface stations at different times of day. The mask in Figure 1b used to separate the 1 km grid into puna, eastern slope and lowlands, was also applied to the ISCCP DX grid. A total of 25 DX grid points were located within the 1×1 degree area. Of these 25, 6 fell within the lowlands area, 6 within the eastern slope area and 11 within the puna, and 2 were excluded from the analysis as they were located on the boundary between the puna and the eastern slope (Figure 4).

3.2.2.1. Mean Annual Cycles

[26] The greatest amplitude seasonal variability occurs on the puna at all times of day from June/July to December/January with an annual range of 0.4 to 0.5, whereas on the eastern slope and the lowlands the range is around 0.2 at 13 LT and 0.3 to 0.4 at 07 and 19 LT.

[27] There is good agreement in the shape and amplitude of the seasonal cycles between MODIS and ISCCP data sets for all zones although the magnitude of the ISCCP cloud frequencies are consistently higher by up to 0.2 (i.e., 20%). The difference is least at 0.1 for the eastern slope from October to March when cloud frequencies reach their maximum. Surface observations from Chontachaca (in the lowlands but close to the base of the eastern slope) closely match the lowland data from ISCCP in terms of mean at 13 LT (Figure 3k). For the eastern slope the ISCCP mean cloud frequencies are approximately 0.1 greater than the Rocotal observations from September to January, but are very similar for other months. The mean values at 07 LT follow a similar pattern in the ISCCP data and observations, although the observations show higher cloud amounts in the dry season for the eastern slope and the lowlands. A similar discrepancy is evident at 19 LT.

[28] In terms of correlation at monthly resolution, as opposed to mean annual cycles, it is less apparent whether ISCCP or MODIS data are more representative of observations (Table 1). ISCCP and MODIS data are strongly correlated for the puna and lowlands, but on the eastern slope correlations are far lower. Similarly, for the ISCCP data and observations, the eastern slope correlations are lower. At 19 LT there is little similarity between ISCCP and observations in terms of mean annual cycles and correlation.

[29] The austral winter minimum in cloud frequency occurs later in the lowlands than on the puna or the eastern slope (Figures 2 and 3). The minimum cloud frequency occurs in June on the puna for all times of the day. In the lowlands it occurs in August/September at 13 LT, in August at 10 LT, in July at 07 LT and in May at 19 LT. However, it should be noted that the 19 LT data are retrieved at nighttime using infrared radiances only, but have been corrected in the ISCCP processing by comparing the differences between daytime visible and infrared radiances [*Rossow and Schiffer*, 1999].

3.2.2.2. Variability in the Mean Annual Cycles

[30] Standard deviations (Figure 3) show a pattern of increased variability at lower mean cloud frequencies (in the dry season) for all times of day on the puna in particular, and to a lesser extent on the eastern slope and lowlands.

[31] A notable difference in variability between the 3 zones is that the magnitude of the standard deviation remains relatively constant at all times of day on the puna and in the lowlands but on the eastern slope, it is much lower at 13 LT than at 19 LT, for example. Highest magnitude peaks in variability occur at 13 LT on the puna, but at 10 LT on the eastern slope and at 07 and 19 LT in the lowlands. The pattern is the same for variability based on daily data for the puna and lowlands (not shown), but for the eastern slope the highest peaks occur at 07 and 19 LT.

[32] In the lowlands at 13 LT (Figure 3k), variability is greater at the start and the end of the dry season in May and September. This pattern is strongest in the MODIS data, but also seen in ISCCP in September and observations in May.

[33] The variability from MODIS and ISCCP is of comparable magnitude for both morning and afternoon data, except in August/September on the eastern slope when ISCCP variance is approximately twice that of MODIS, and in May in the lowlands when the opposite occurs. Very large variances occur in May and June in the 13 LT observations, which are approximately twice those of the ISCCP data. The occurrence of large differences in variance was considered too infrequent to be significant.

3.2.3. Diurnal Cycles by Season on Puna, Eastern Slope and Lowlands

[34] To examine the variation in the diurnal cycle for the three zones by month, a time series of cloud frequency for each zone from the ISCCP data set was extracted from a 1×1 degree square as in Figure 3. In all zones, the amplitude of the diurnal cycle is reduced during the wet season, particularly from December to March (Figure 5). During this period, cloud frequencies in all zones range between approximately 0.7 and 0.9 throughout the diurnal cycle, whereas in June, the amplitude of the diurnal cycle is approximately 0.4. In the dry season there is a more marked increase at sunrise (07 LT), with a peak at 13 or 16 LT and relatively constant low values from

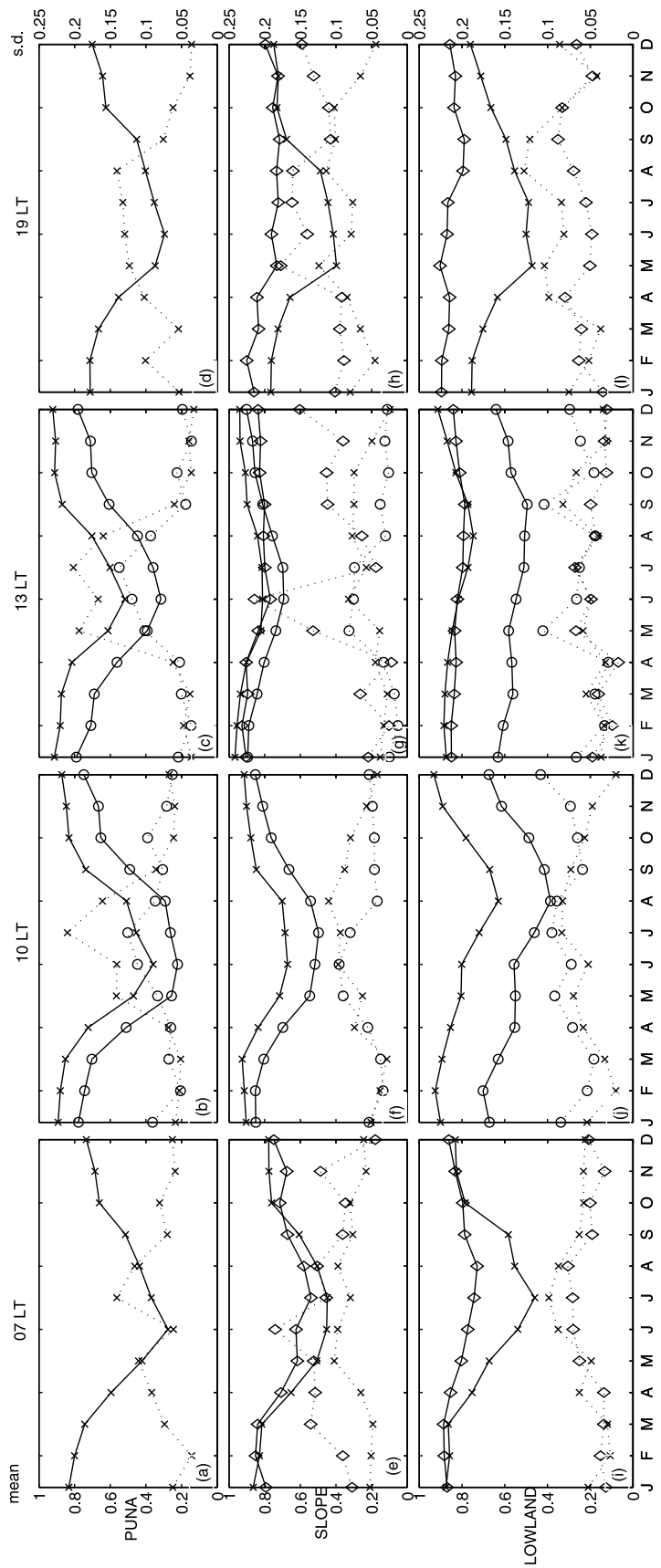

Figure 3. Comparison of mean annual cycle of cloud frequency (solid lines) between ISCCP DX (2000–2008) (crosses), MODIS MOD35 (circles) and surface observations (diamonds) from puna at (a) 07 LT, (b) 09 or 10 LT, (c) 13 or 14 LT and (d) 19 LT and eastern slope at (e) 07 LT, (f) 09 or 10 LT, (g) 13 or 14 LT and (h)19 LT, and lowlands at (i) 07 LT, (j) 09 or 10 LT, (k) 13 or 14 LT and (l) 19 LT. Standard deviations based on monthly data are shown by dotted lines.

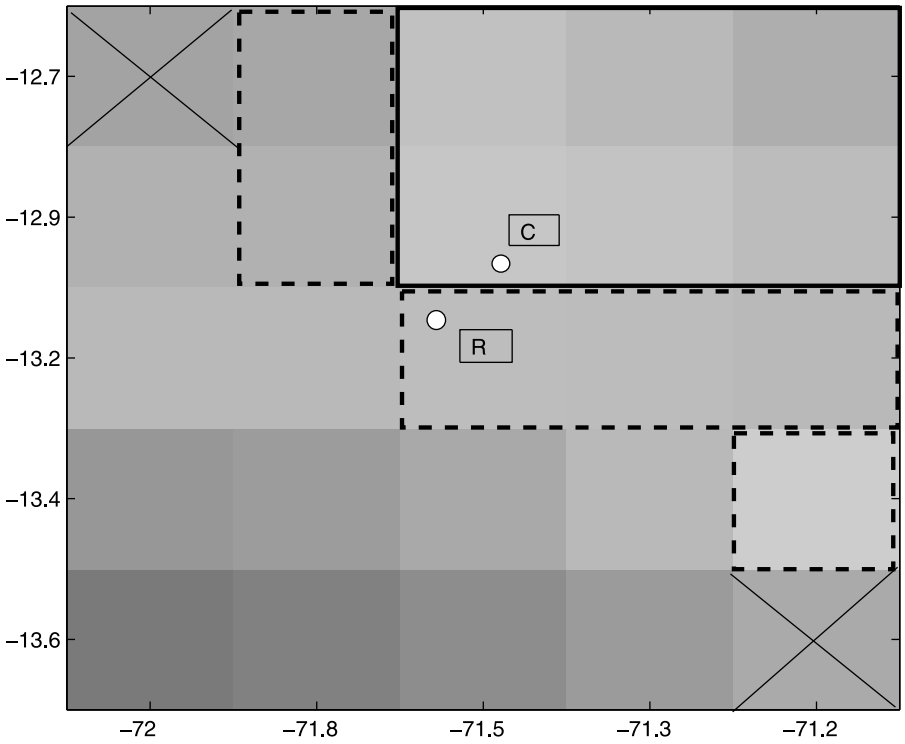

Figure 4. ISCCP grid showing pixels assigned to lowlands enclosed by a solid line, pixels assigned to eastern slope enclosed by a dotted line. The remaining pixels were assigned to puna. Crosses indicate pixels there were not included in the analysis. 'C' indicates location of Chontachaca weather station and 'R' the Rocotal station.

19 LT and overnight. In the wet season in the lowlands and on the eastern slope there is a more gradual increase from 19 LT and overnight until 13 LT.

[35] For most months, and throughout the diurnal cycle, puna cloud frequencies are less than those of the other two zones, with a maximum difference in June. However, in September and October, they exceed those in the lowlands at 10 and 13 LT. Eastern slope cloud frequencies are mostly similar or greater than those in the lowlands but from April to June, lowland values exceed those on the eastern slope from 07 to 10 LT.

4. Discussion

4.1. Low-Level Circulation and Mean Annual Cloud Frequency

[36] The high mean annual cloud frequencies on the eastern slope relative to those on the puna and lowlands are attributable to the prevailing easterly trade winds. . Streamlines from NCEP/NCAR reanalysis (Figure 6) show air arriving at the study area travels over Amazonia throughout the year, with a mean wind direction between easterly and northwesterly, thus maintaining the moisture flux to the eastern slope. In addition, the angle of incidence of the prevailing winds with the eastern slope may help to maintain the high cloud frequency during the dry season, as during these months, as it is approximately perpendicular to the slope (Figure 6b). Although the spatial resolution of the reanalysis is 2.5 degrees, it is appropriate for examining large-scale flow. According to the findings of *Nair et al.* [2008] with respect to the Monteverde cloud forest, areas of cloud immersion are more fragmented where winds are parallel to the slope as opposed to perpendicular. *Killeen et al.* [2007] also suggest that the interaction of topography and low-level flow, in this case, the SALLJ, explains the existence of four "wet spots" along the eastern side of the Andes, based on precipitation data and wet season cold cloud frequency. One such area coincides with the study area. The extensive band of high cloud frequency was also identified in rainfall climatology [*de Angelis et al.*, 2004; *Negri et al.*, 2000] and in the cloud climatology of Ecuador [*Bendix et al.*, 2004, 2006]. The altitude range of the band is similar to that found on the eastern slopes in the Andes in Ecuador, but the altitude of maximum

Table 1. Correlation Coefficients and Associated p Values of Cloud Frequency Anomalies From ISCCP, MODIS MOD35 Visible Cloud Flags and Ground-Based Observations for Puna, Eastern Slope and Lowlands[a]

	Puna		Eastern Slope				Lowlands			
	10 LT	13 LT	07 LT	10 LT	13 LT	19 LT	07 LT	10 LT	13 LT	19 LT
ISCCP/MODIS										
r	0.804	0.681		0.457	0.299			0.637	0.493	
p	0.000	0.000		0.000	0.015			0.000	0.000	
ISCCP/OBS										
r			0.512		0.348	0.047	0.382		0.461	0.089
p			0.000		0.004	0.706	0.002		0.000	0.478
MODIS/OBS										
r				0.287				0.625		
p					0.020				0.000	

[a]Includes only time periods common to all data sets.

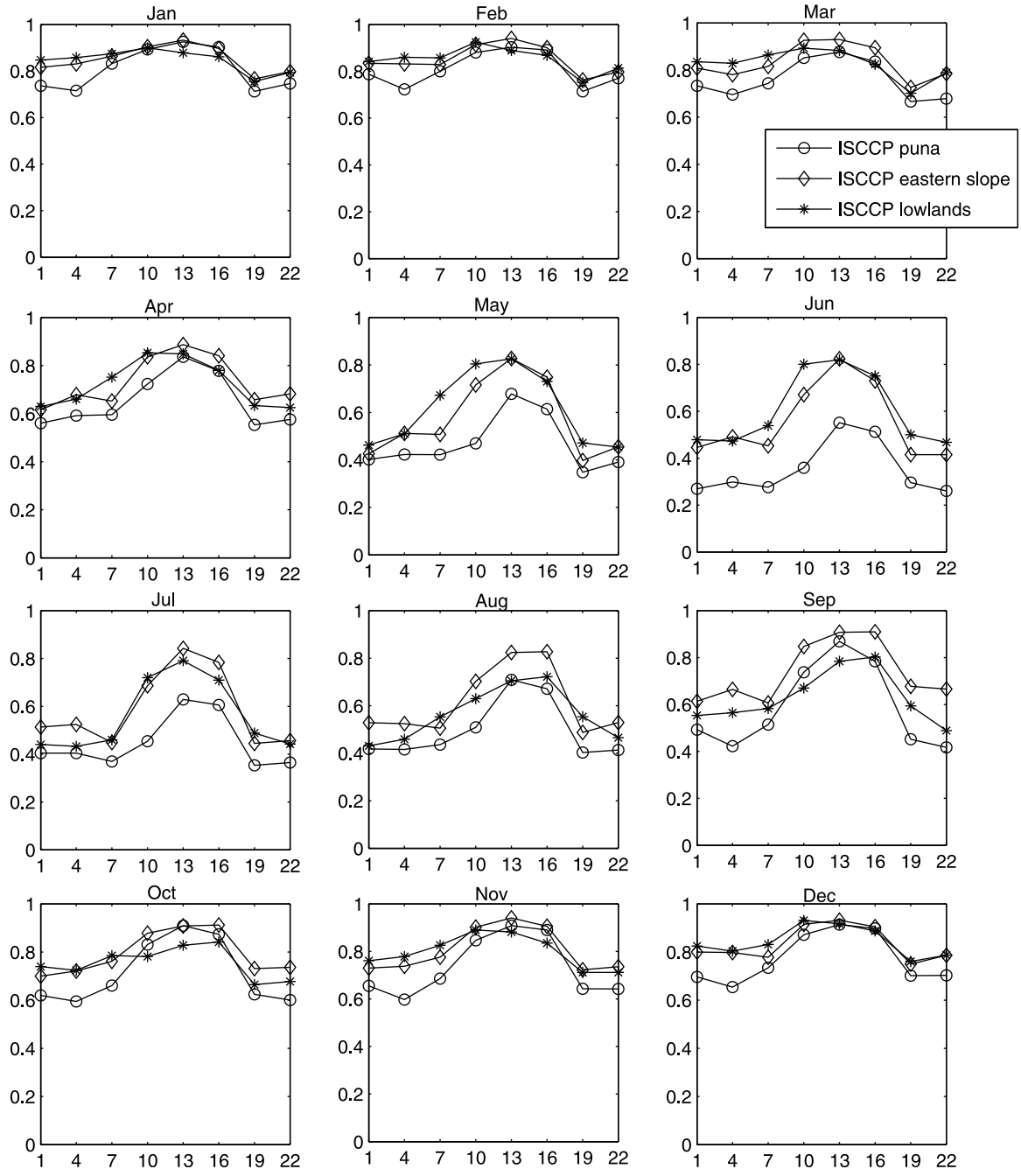

Figure 5. Diurnal cycle (times are in local time or UTC-5) of cloud frequency by month from ISCCP DX data 2000–2008 for puna, eastern slope and lowlands.

cloud frequency is lower in this study (2000 to 3500 m as opposed to 3200 to 4000 m in Ecuador). However, the high resolution climatology in Figure 2 is based on daytime data only, which could explain the difference.

[37] The maintenance of upslope flow by more localized diurnal circulations that arise from differential heating of the slope and the free troposphere above, as suggested in modeling studies of the Altiplano by *Garreaud* [1999], is also likely to be a factor in the high cloud frequencies on the eastern slope.

4.2. Seasonal Cycles and Atmospheric Circulation

[38] The seasonal cycle in the study area contrasts with that in Ecuador [*Bendix et al.*, 2006] in that pronounced cloud frequency minima occur in winter in the study area but in Ecuador they remain high or reach secondary maxima. This may be attributed to an increase in the strength of easterlies in winter [*Bendix et al.*, 2006].

[39] The annual cycle of upper level zonal flow from NCEP-NCAR reanalysis (Figures 7 and 8) helps to explain some features of the seasonal cycle of cloud frequency.

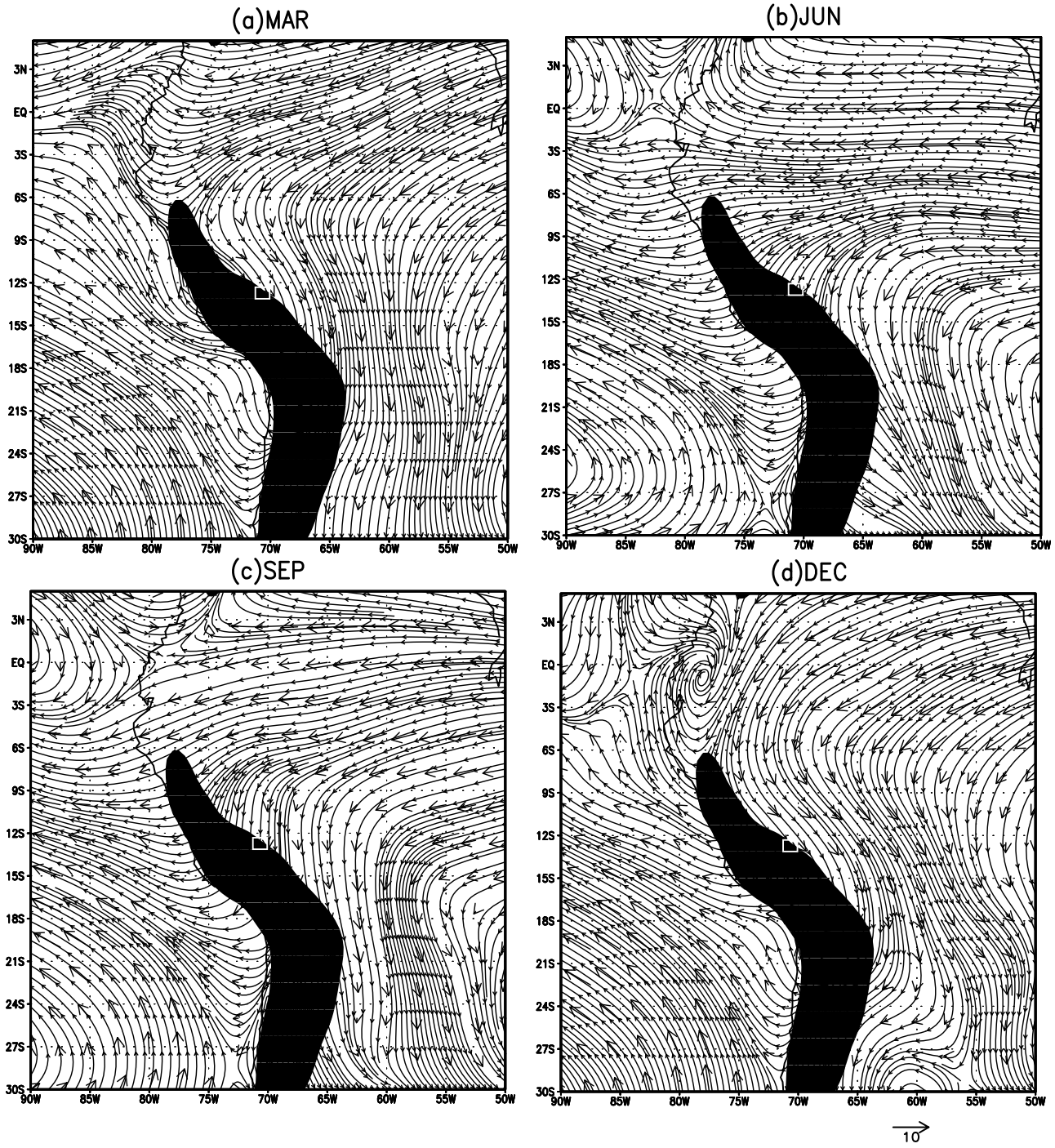

Figure 6. Mean 850 hPa streamlines (corresponding to approximately1500 m elevation) and wind vectors from NCEP/NCAR reanalysis 2000–2008 for (a) March, (b) June, (c) September and (d) December. One degree × 1 degree box containing study area is marked. Terrain above 1500 m elevation is masked out.

At upper levels in summer (DJF), the formation of the Bolivian high causes a reversal in mid and upper level wind direction in southern Peru and the surrounding regions. Upper level winds are easterly from January to March (Figure 8) when the Bolivian high is centered to the south of the study area. In the central Andes region in summer, easterlies are associated with moist mid-level flow from the Amazon which enhances convection and cloud formation [e.g., *Garreaud and Aceituno*, 2001]. However, it cannot be assumed that the same is true in winter: the sign of correlation between cloud frequency and upper level u and v winds components (not shown) changes from summer to winter. This association of increased cloud frequency with upper westerlies in winter requires further investigation.

[40] A key difference between the three zones is the greater amplitude annual cycles on the puna, with lower

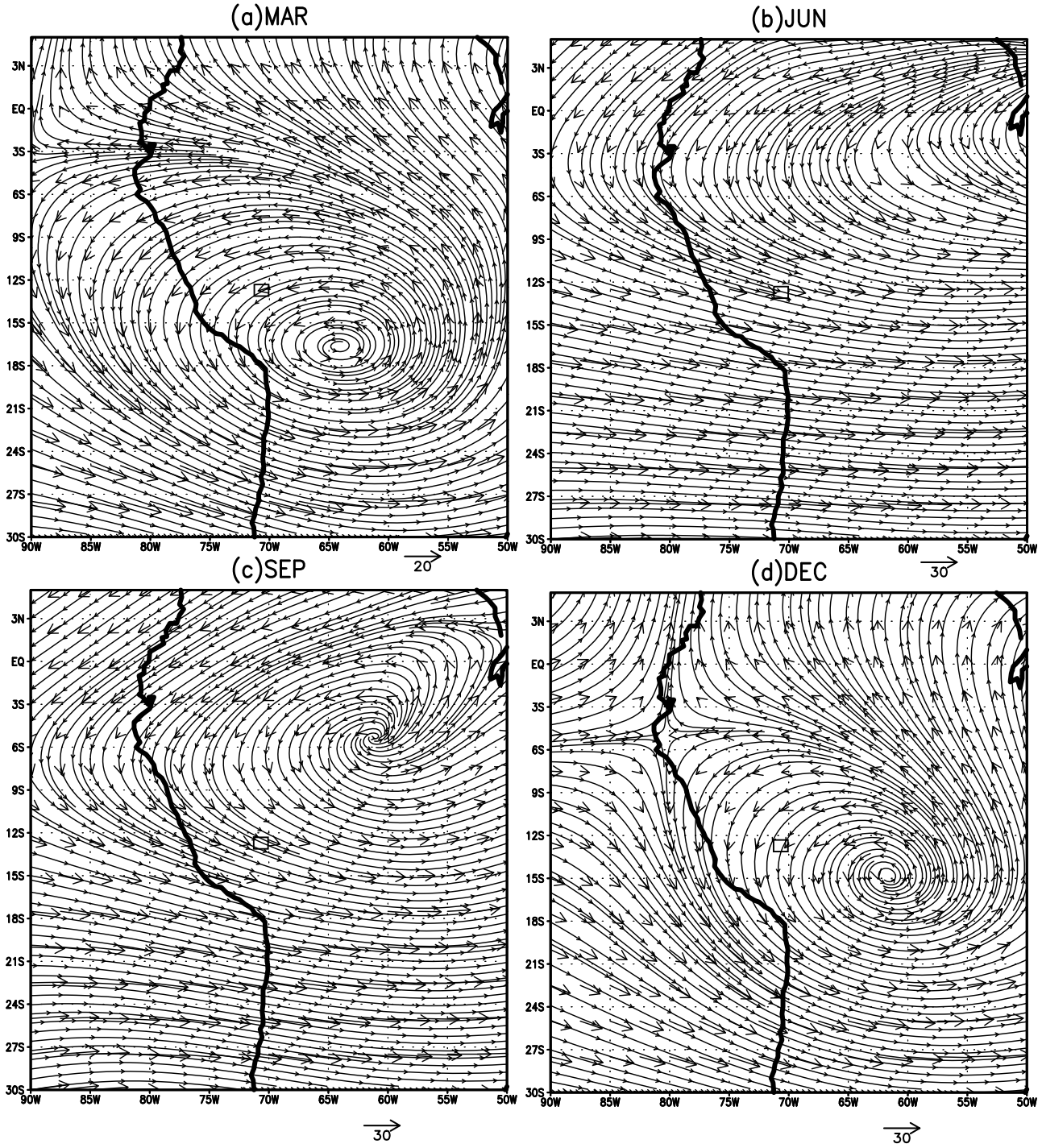

Figure 7. Mean 200 hPa streamlines and wind vectors from NCEP-NCAR reanalysis data 2000–2008 for (a) March, (b) June, (c) September and (d) December. One degree × 1 degree box containing study area is marked.

cloud frequencies and higher variability in the dry season compared with the other zones. The puna is a drier environment and therefore more reliant on external moisture to initiate convection. *Garreaud* [1999, 2000] note that a lifting mechanism and boundary layer moisture are required for convection, and that on the Altiplano, convection depends on upslope moisture transport. It has been found that intraseasonal variability has more effect on the puna in the dry season, and in the case of midlatitude cold incursions, can be associated with temperature inversions that limit vertical cloud growth (K. Halladay et al., Atmospheric structure and cloud depth in a tropical montane cloud forest, submitted to *Atmospheric Research*, 2012).

[41] Another difference is that the minimum in cloud frequency occurs earlier in the dry season on the puna. The late dry season minimum seen in the ISCCP data is supported by

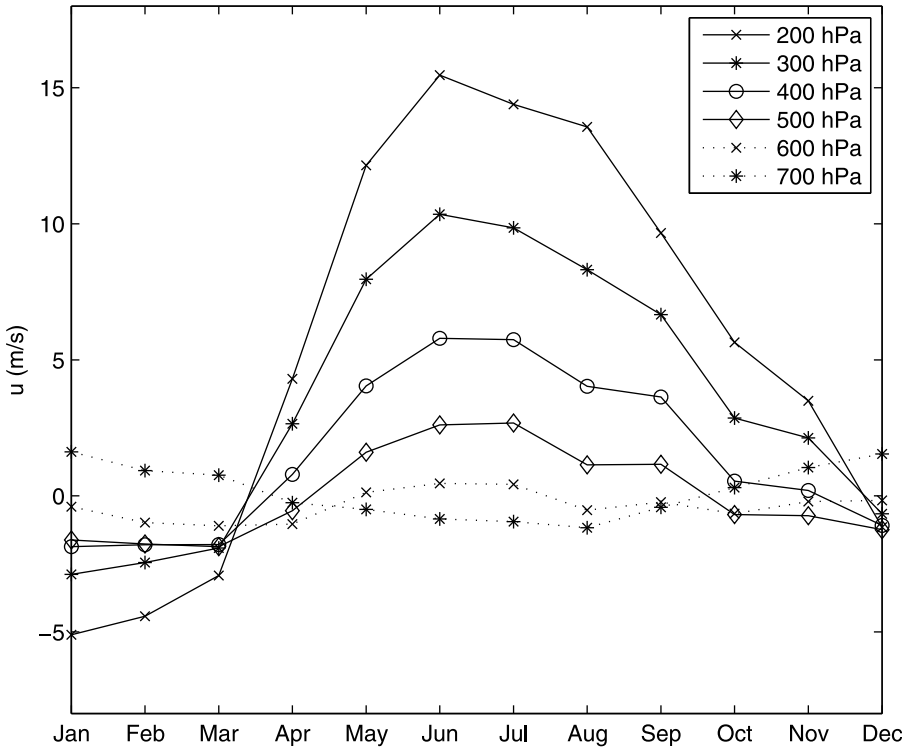

Figure 8. Mean zonal wind in m/s from NCEP-NCAR reanalysis for region bounded by 75°W, 70°W, 15°S, 10°S for the period 1983 to 2008 at levels: 200 hPa, 300 hPa, 400 hPa, 500 hPa, 600 hPa, and 700 hPa.

mean annual cycles of relative humidity measured at the Rocotal and Chontachaca stations from 2000 to 2006, which also show that the minimum occurs in September (it is assumed that relative humidity is highly correlated with cloud frequency). This may be another indication of the reliance of the puna on external moisture sources. *Nair et al.* [2008] report that soil moisture influences variability of cloud base height from year to year in the Monteverde cloud forest, thus it could feasibly influence the annual cycle of cloud frequency in a region such as the study area which has pronounced wet and dry seasons. Hence, the depleted moisture flux from the Trades in austral winter would not become limiting in the lowlands until the late dry season. However, the puna would be affected by this almost immediately.

[42] The question remains as to why cloud frequencies on the puna start to increase in September, while at the same time reaching a minimum on the lowlands. Incident solar radiation increases from June to September but this would be expected to increase cloud frequencies in all zones. In austral summer, upper easterlies are correlated with increased cloud frequency, but in September which is transitional, there is no correlation for lowlands and eastern slope and it is weak for the puna (not shown). This suggests that the upper air circulation is not a factor. Figure 8 shows little difference in zonal wind between 600 and 700 hPa (separating upper and mid elevations in the study area) in September. The increase on the puna could be the result of convergence of westerlies with strong upslope flow developing on the slope from increased insolation, as has been described for the Altiplano [*Garreaud*, 1999] but further investigation would be required to confirm this.

4.3. Local Circulations and Low-Level Convergence

[43] Daytime easterly upslope flow and nighttime westerly downslope flow may explain many of the differences in seasonal cycles between the three zones of the study area at different times of the day. Katabatic (downslope) flows have been observed on eastern slopes in Ecuador [*Bendix et al.*, 2009; *Trachte et al.*, 2010] and according to modeling studies by *Garreaud* [1999], westerly downslope flow from the Altiplano over the eastern slope toward the lowlands begins soon after sunset and persists into the early morning. Evidence for this in the study area has been found in dry season vertical wind profiles from the Kosñipata Valley (Halladay et al., submitted manuscript, 2012).

[44] Low-level convergence of downslope flows and synoptic easterlies at the base of the slope promotes uplift and cloud formation [*Bendix et al.*, 2009; *Garreaud and Wallace*, 1997; *Giovannettone and Barros*, 2009], and is likely to be the dominant cloud formation mechanism at lower elevations in the absence of diurnal heating. *Giovannettone and Barros* [2009] report that the peak in convective cloud formation based on wet season data occurs at 1000–2000 m, which corresponds to the eastern slope. However, the location of convergence and therefore cloud formation may vary both seasonally and intraseasonally with the synoptic easterlies and the westerly downslope flow. Both *Giovannettone and Barros* [2009] and *Garreaud and Wallace* [1997] found nocturnal maxima though both used infrared data which detects only deep cloud so may have missed orographic cloud with lower top heights forming through upslope flow in the daytime. This may explain why daytime maxima were

found in this study. Nocturnal maxima were also found in Ecuador [*Bendix et al.*, 2004], using a method that could detect low cloud, though there are substantial differences in atmospheric circulation between this site in Ecuador and the study area.

[45] The diurnal cycles of upslope and downslope flows further south on the eastern edge of the Altiplano at 16°S modeled by *Garreaud* [1999], for wet (dry) episodes during the wet season, exhibited intraseasonal variability associated with upper-level easterly(westerly) anomalies. At an elevation of 1500 m, the change from downslope to upslope flows occurred at 07 LT with upper easterly anomalies, but with upper westerly anomalies it occurred at 11 LT [*Garreaud*, 1999]. Upper-level easterly/westerly anomalies could also affect flows on the eastern slope in the dry season, although in the dry season westerlies are correlated with increased cloud frequency. Upper westerly anomalies would enhance downslope flow leading to increased low-level convergence with synoptic easterlies and convection.

[46] At 13 LT, convection resulting from diurnal heating, as opposed to low-level convergence, would be the dominant cloud formation mechanism in all zones, though it may be modulated by boundary layer moisture levels. This could explain why at 13 LT the cloud frequency minimum in the lowlands occurs later in the dry season than for 07 LT (Figure 3). On the puna the minimum occurs in the same month for all times of day as it is likely to be more affected by diurnal heating rather than other mechanisms such as low-level convergence. Peak variability also occurs at 13 LT on the puna, which may be because the strength and occurrence of upslope flow at this time of day, modulated by upper-level circulation, adds an extra component of variability, whereas at 07 and 19 LT local circulations would be weak or absent. Lowest variability at 13 LT on the eastern slope may be due to orographic lifting in addition to persistent upslope flow at this level which help to maintain consistently high cloud frequencies. Cloud frequency variability at 07 and 19 LT on the eastern slope and lowlands may be subject to variations in the timing of the switch from upslope to downslope flow.

4.4. ISCCP, MODIS and Observations

[47] ISCCP cloud frequencies were consistently higher than those from MODIS. Aside from differences in the algorithm and sensors, this may be attributed to the use of MODIS visible cloud flags in an uncalibrated form to estimate cloud frequency. As noted by *Kotarba* [2010], the cloud mask is not necessarily a measure of cloud frequency and may need to be calibrated to obtain absolute cloud amounts. However, the purpose of this study is to determine the relative changes in cloud frequency on seasonal and diurnal timescales, and spatially between the three zones. Therefore, absolute measures are less important. The magnitude of this bias is relatively constant throughout the annual cycle for the puna (0.1) and lowlands (0.2), which suggests that the difference in detection method is insensitive to variations in cloud amount and type within a zone (e.g., lowlands, puna) through the annual cycle. The bias does vary through the annual cycle for the eastern slope but this is likely to result from the very high cloud frequencies, indicating many fully cloudy fields of view, in which case there would be no difference in the amount of cloud detected between the two approaches.

[48] The similarity between the surface observations and the ISCCP data at 13 LT is surprising given that surface observations of cloud from a point location tend to overestimate compared with satellite estimates, especially at low latitudes [*Malberg*, 1973]. However, it strengthens the case for the use of the ISCCP DX data in differentiating between the cloud climatologies of the three zones and examining their temporal variability.

[49] Some large differences were found between the ISCCP data and observations at 07 and 19 LT (up to 0.4). This may be an artifact of the comparison between data from an area and point observations, for example, Chontachaca is located close to the eastern slope and may therefore reflect cloudier conditions than the wider lowlands zone. This would be less significant in the wet season as the areas of high cloud frequency are more extensive, i.e., less restricted to the eastern slope. The occurrence of this bias at 07 and 19 LT and not at 13 LT may be attributed to the typical location of cloud at this time of day, in that it may be more localized over the observation station rather than over the zone as a whole. Differences could also result from the effect of darkness on the ability of an observer to estimate cloud cover, or on the amount of cloud detected by the ISCCP algorithm which includes the visible channel, which would be more marked in austral winter when day length is slightly less. This may contribute to the low correlation between observations and ISCCP data at 19 LT. Errors also arise from the perception or skill of observers in estimating cloud cover in oktas, and missing data in the case of the Rocotal station. As a result of these discrepancies, the conclusions drawn for 07 and 19 LT are treated with caution.

5. Summary and Conclusions

[50] The mean cloud frequency, seasonal and diurnal cycles of cloud frequency at the Andes/Amazon transition in southeastern Peru have been examined with the aid of satellite-derived cloud mask products from ISCCP and MODIS, and ground-based observations from two stations. The objectives were to describe the cloud climatology of the study area in the regional context, examine the differences in seasonal and diurnal cycles between the three zones and relate all to the large-scale circulation and cloud formation mechanisms.

[51] Our main conclusions are:

[52] (1) MODIS MOD35 data showed that the eastern slope is a region of high cloud frequency (>0.65). It is part of a band of high cloud frequency which persists through all seasons, and maintains higher cloud frequency than other areas on the slope. The slope also experiences lower cloud frequency variability than the surrounding areas. The persistent high cloud frequency and low variability is likely to result from the mean low-level wind trajectory, its angle of incidence, and diurnal upslope flow.

[53] (2) All three zones showed reduced cloud frequency in austral winter using ISCCP DX and MODIS MOD35 data, but the highest amplitude seasonal cycle was found on the puna region. This may be attributed to a greater reliance on external moisture sources.

[54] (3) The minimum cloud frequency was found to occur in June on the puna and the eastern slope but for the lowlands it occurred later (July at 07 LT and in August at 10 LT and 13 LT). A possible explanation for this is a greater

moisture supply from evapotranspiration at the start versus the end of the dry season in the lowlands.

[55] (4) Cloud variability is higher on the puna in the dry season when mean cloud frequencies are lower. The same pattern occurs on the eastern slope and in the lowlands but is less marked. The higher variability may be associated with a dependence on upslope moisture transport for cloud formation on the puna, which is subject to variability in upper and mid-level zonal winds.

[56] (5) Variability is lowest at 13 LT on the eastern slope but increases at 07 and 19 LT, but for other zones it remains relatively constant at all times of day. This may be caused by diurnal heating leading to persistent upslope flow and convection.

[57] (6) In all zones the amplitude of the diurnal cycle using ISCCP DX data increased from approximately 0.2 to 0.4 from the wet to the dry season. Absolute values are lower on the puna in most months than in the other two zones, with the maximum difference between the three zones in June.

[58] (7) Lowland and eastern slope cloud frequencies exceed those on the puna in the early hours in the wet season, which may be attributable to low-level convergence at lower altitudes.

[59] (8) ISCCP and MODIS data reproduced the same features of the mean annual cycles of cloud frequency at 10 and 13 LT in all zones despite the considerable differences in spatial resolution, although the absolute values from ISCCP were consistently higher by up to 20%.

[60] (9) ISCCP cloud frequencies were more similar to surface observations than those from MODIS in terms of absolute magnitude.

[61] This study has demonstrated the usefulness of satellite data in characterizing the cloud climatology even for small areas in complex terrain, which is encouraging for the monitoring of cloud frequency as the length of the satellite data record and resolution improve. We have shown that there are differences in the cloud frequency climatology in terms of mean cycles and variability between the three zones in the study area, which suggest different levels of vulnerability owing to the relative dominance of various cloud formation mechanisms. Some of these mechanisms may be affected by climate change, as it is likely to influence dry season intensity and length [*Cox et al.*, 2008; *Malhi et al.*, 2009] which would in turn affect moisture availability in the boundary layer, and upper level zonal flow (through ENSO or other SST-related mechanisms).

[62] The results indicate that in this area, it is likely that an assessment of the impact of climate change requires more than a consideration of the effect of surface temperature increases on the LCL to predict future cloud patterns. A study to test the sensitivity of cloud formation to changes in variables such as upper level zonal flow, synoptic easterlies and dry season intensity would be the logical next step. A companion paper [*Halladay et al.*, 2012] focuses on long-term trends in cloud frequency based on ISCCP data, and explores possible large-scale controlling mechanisms.

[63] **Acknowledgments.** KH is funded by a studentship from the UK Natural Environment Research Council (NERC: NE/F00916X/1) and work in Peru was supported by the John Fell Fund. We thank N. Salinas Revilla, R. Chacon Campana, Z. Huaman Gutierrez (Senamhi, Cuzco), and for their assistance with logistics and access to meteorological data.

References

Ackerman, S., K. Strabala, P. Menzel, R. Frey, C. Moeller, L. Gumley, B. Baum, S. Wetzel Seemann, and H. Zhang (2006), Discriminating clear-sky from cloud with MODIS Algorithm Theoretical Basis Document (MOD35), Coop. Inst. for Meteorol. Stud., Univ. of Wis., Madison.

Bendix, J., R. Rollenbeck, and W. E. Palacios (2004), Cloud detection in the tropics—A suitable tool for climate-ecological studies in the high mountains of Ecuador, *Int. J. Remote Sens.*, *25*(21), 4521–4540, doi:10.1080/01431160410001709967.

Bendix, J., R. Rollenbeck, D. Gottlicher, and J. Cermak (2006), Cloud occurrence and cloud properties in Ecuador, *Clim. Res.*, *30*(2), 133–147, doi:10.3354/cr030133.

Bendix, J., K. Trachte, J. Cermak, R. Rollenbeck, and T. Nauss (2009), Formation of convective clouds at the foothills of the tropical eastern Andes (south Ecuador), *J. Appl. Meteorol. Climatol.*, *48*(8), 1682–1695, doi:10.1175/2009JAMC2078.1.

Campbell, G. G. (2004), View angle dependence of cloudiness and the trend in ISCCP cloudiness, paper presented at 13th Conference on Satellite Meteorology and Oceanography, Am. Meteorol. Soc., Norfolk, Va.

Cox, P. M., P. P. Harris, C. Huntingford, R. A. Betts, M. Collins, C. D. Jones, T. E. Jupp, J. A. Marengo, and C. A. Nobre (2008), Increasing risk of Amazonian drought due to decreasing aerosol pollution, *Nature*, *453*(7192), 212–215, doi:10.1038/nature06960.

de Angelis, C. F., G. R. McGregor, and C. Kidd (2004), A 3 year climatology of rainfall characteristics over tropical and subtropical South America based on Tropical Rainfall Measuring Mission precipitation radar data, *Int. J. Climatol.*, *24*(3), 385–399, doi:10.1002/joc.998.

Evan, A. T., A. K. Heidinger, and D. J. Vimont (2007), Arguments against a physical long-term trend in global ISCCP cloud amounts, *Geophys. Res. Lett.*, *34*, L04701, doi:10.1029/2006GL028083.

Foster, P. N. (2001), The potential negative impacts of climate change on tropical montane cloud forests, *Earth Sci. Rev.*, *55*, 73–106, doi:10.1016/S0012-8252(01)00056-3.

Garreaud, R. D. (1999), Multiscale analysis of the summertime precipitation over the central Andes, *Mon. Weather Rev.*, *127*(5), 901–921, doi:10.1175/1520-0493(1999)127<0901:MAOTSP>2.0.CO;2.

Garreaud, R. D. (2000), Intraseasonal variability of moisture and rainfall over the South American Altiplano, *Mon. Weather Rev.*, *128*(9), 3337–3346, doi:10.1175/1520-0493(2000)128<3337:IVOMAR>2.0.CO;2.

Garreaud, R. D., and P. Aceituno (2001), Interannual rainfall variability over the South American Altiplano, *J. Clim.*, *14*(12), 2779–2789, doi:10.1175/1520-0442(2001)014<2779:IRVOTS>2.0.CO;2.

Garreaud, R. D., and J. M. Wallace (1997), The diurnal march of convective cloudiness over the Americas, *Mon. Weather Rev.*, *125*(12), 3157–3171, doi:10.1175/1520-0493(1997)125<3157:TDMOCC>2.0.CO;2.

Giovannettone, J. P., and A. P. Barros (2009), Probing regional orographic controls of precipitation and cloudiness in the central Andes using satellite data, *J. Hydrometeorol.*, *10*(1), 167–182, doi:10.1175/2008JHM973.1.

Halladay, K., M. New, and Y. Malhi (2012), Cloud frequency climatology at the Andes/Amazon transition: 2. Trends and variability, *J. Geophys. Res.*, *117*, D23103, doi:10.1029/2012JD017789.

Horel, J. D., A. N. Hahmann, and J. E. Geisler (1989), An investigation of the annual cycle of convective activity over the tropical Americas, *J. Clim.*, *2*(11), 1388–1403, doi:10.1175/1520-0442(1989)002<1388:AIOTAC>2.0.CO;2.

Hubanks, P. A., M. D. King, S. Platnick, and R. A. Pincus (2008), MODIS Atmosphere L3 Gridded Product Algorithm Theoretical Basis Document, NASA Goddard Space Flight Cent., Greenbelt, Md.

Joyce, R., J. Janowiak, and G. Huffman (2001), Latitudinally and seasonally dependent zenith-angle corrections for geostationary satellite IR brightness temperatures, *J. Appl. Meteorol.*, *40*(4), 689–703, doi:10.1175/1520-0450(2001)040<0689:LASDZA>2.0.CO;2.

Kalnay, E., et al. (1996), The NCEP/NCAR 40-year reanalysis project, *Bull. Am. Meteorol. Soc.*, *77*(3), 437–471, doi:10.1175/1520-0477(1996)077<0437:TNYRP>2.0.CO;2.

Karmalkar, A. V., R. S. Bradley, and H. F. Diaz (2008), Climate change scenario for Costa Rican montane forests, *Geophys. Res. Lett.*, *35*, L11702, doi:10.1029/2008GL033940.

Killeen, T. J., M. Douglas, T. Consiglio, P. M. Jorgensen, and J. Mejia (2007), Dry spots and wet spots in the Andean hotspot, *J. Biogeogr.*, *34*(8), 1357–1373, doi:10.1111/j.1365-2699.2006.01682.x.

Kotarba, A. Z. (2010), Estimation of fractional cloud cover for Moderate Resolution Imaging Spectroradiometer/Terra cloud mask classes with high-resolution over ocean ASTER observations, *J. Geophys. Res.*, *115*, D22210, doi:10.1029/2009JD013520.

Lenters, J. D., and K. H. Cook (1999), Summertime precipitation variability over South America: Role of the large-scale circulation, *Mon. Weather Rev.*, *127*(3), 409–431, doi:10.1175/1520-0493(1999)127<0409:SPVOSA>2.0.CO;2.

Malberg, H. (1973), Comparison of mean cloud cover obtained by satellite photographs and ground-based observations over Europe and Atlantic, *Mon. Weather Rev.*, *101*, 893–897, doi:10.1175/1520-0493(1973)101<0893:COMCCO>2.3.CO;2.

Malhi, Y., L. Aragao, D. Galbraith, C. Huntingford, R. Fisher, P. Zelazowski, S. Sitch, C. McSweeney, and P. Meir (2009), Exploring the likelihood and mechanism of a climate-change-induced dieback of the Amazon rainforest, *Proc. Natl. Acad. Sci. U. S. A.*, *106*(49), 20,610–20,615, doi:10.1073/pnas.0804619106.

Malhi, Y., M. Silman, N. Salinas, M. Bush, P. Meir, and S. Saatchi (2010), Introduction: Elevation gradients in the tropics: Laboratories for ecosystem ecology and global change research, *Global Change Biol.*, *16*(12), 3171–3175, doi:10.1111/j.1365-2486.2010.02323.x.

Minnis, P. (1989), Viewing zenith angle dependence of cloudiness determined from coincident GOES East and GOES West data, *J. Geophys. Res.*, *94*(D2), 2303–2320, doi:10.1029/JD094iD02p02303.

Nair, U. S., S. Asefi, R. M. Welch, D. K. Ray, R. O. Lawton, V. S. Manoharan, M. Mulligan, T. L. Sever, D. Irwin, and J. A. Pounds (2008), Biogeography of tropical montane cloud forests. Part II: Mapping of orographic cloud immersion, *J. Appl. Meteorol. Climatol.*, *47*(8), 2183–2197, doi:10.1175/2007JAMC1819.1.

Negri, A. J., E. N. Anagnostou, and R. F. Adler (2000), A 10-yr climatology of Amazonian rainfall derived from passive microwave satellite observations, *J. Appl. Meteorol.*, *39*(1), 42–56, doi:10.1175/1520-0450(2000)039<0042:AYCOAR>2.0.CO;2.

Pinto, E., Y. Shin, S. A. Cowling, and C. D. Jones (2009), Past, present and future vegetation-cloud feedbacks in the Amazon Basin, *Clim. Dyn.*, *32*(6), 741–751, doi:10.1007/s00382-009-0536-5.

Pounds, J. A., M. P. L. Fogden, and J. H. Campbell (1999), Biological response to climate change on a tropical mountain, *Nature*, *398*(6728), 611–615, doi:10.1038/19297.

Rapp, J., and M. Silman (2012), Diurnal, seasonal and altitudinal trends in microclimate across a 3900 meter altitudinal gradient in the humid tropics, *Clim. Res.*, in press.

Rossow, W. B., and L. C. Garder (1993), Cloud detection using satellite measurements of infrared and visible radiances for ISCCP, *J. Clim.*, *6*(12), 2341–2369, doi:10.1175/1520-0442(1993)006<2341:CDUSMO>2.0.CO;2.

Rossow, W. B., and R. A. Schiffer (1991), ISCCP cloud data products, *Bull. Am. Meteorol. Soc.*, *72*(1), 2–20, doi:10.1175/1520-0477(1991)072<0002:ICDP>2.0.CO;2.

Rossow, W. B., and R. A. Schiffer (1999), Advances in understanding clouds from ISCCP, *Bull. Am. Meteorol. Soc.*, *80*(11), 2261–2287, doi:10.1175/1520-0477(1999)080<2261:AIUCFI>2.0.CO;2.

Still, C. J., P. N. Foster, and S. H. Schneider (1999), Simulating the effects of climate change on tropical montane forests, *Nature*, *398*, 608–610, doi:10.1038/19293.

Trachte, K., R. Rollenbeck, and J. Bendix (2010), Nocturnal convective cloud formation under clear-sky conditions at the eastern Andes of south Ecuador, *J. Geophys. Res.*, *115*, D24203, doi:10.1029/2010JD014146.

Vuille, M. (1999), Atmospheric circulation over the Bolivian Altiplano during dry and wet periods and extreme phases of the Southern Oscillation, *Int. J. Climatol.*, *19*(14), 1579–1600, doi:10.1002/(SICI)1097-0088(19991130)19:14<1579::AID-JOC441>3.0.CO;2-N.

Vuille, M., and F. Keimig (2004), Interannual variability of summertime convective cloudiness and precipitation in the central Andes derived from ISCCP-B3 data, *J. Clim.*, *17*(17), 3334–3348, doi:10.1175/1520-0442(2004)017<3334:IVOSCC>2.0.CO;2.

Vuille, M., D. R. Hardy, C. Braun, F. Keimig, and R. S. Bradley (1998), Atmospheric circulation anomalies associated with 1996/1997 summer precipitation events on Sajama ice cap, Bolivia, *J. Geophys. Res.*, *103*(D10), 11,191–11,204, doi:10.1029/98JD00681.